EXTENDED ABSTRACT

Accelerated circadian cycles of photoperiod favor photosynthetic efficiency and growth in grapevine

Mariana G. Tournier[1,2], Laurent Torregrosa[3], Jana Kändler[4], Romain Boulord[3], Anna Medici[5], Anne Pellegrino[3]
*Corresponding author: anne.pellegrino@institut-agro.fr

[1] EEA, INTA, Luján de Cuyo, Mendoza, Argentina
[2] CONICET, Ciudad autónoma de Buenos Aires, Buenos Aires, Argentina
[3] LEPSE, Montpellier University, CIRAD, INRAE, Institut Agro, Montpellier, France
[4] Dept Sci. & Educ. in Vine and Wine, Institut Agro, Montpellier, France
[5] IPSiM, Montpellier Uni, CNRS, INRAE, Institut Agro, Montpellier, France

Keywords: *Vitis vinifera*, microvine, urban agriculture, radiation and water use efficiency

INTRODUCTION

Climate change presents a challenge for agriculture worldwide. Yet, crop productivity is negatively impacted by abiotic hazards such as high temperatures and water deficit. In this context, agricultural production is shifting towards areas either of higher altitude or latitude, to lower crop exposure to such constraints (Muluneh, 2021). Meanwhile, the expansion of urban areas reduces the availability of arable land and represents a threat to food sustainability. To increase the efficiency of agricultural systems, artificial devices in urban area including growth chambers and greenhouses deserve more attention. Light intensity, spectrum and duration are essential factors for plant productivity under indoor growing conditions, to which the circadian rhythm must also be added (Paradiso & Proietti, 2021).

In plants, the photoperiod duration and the circadian rhythms regulate various processes such as stomatal opening and growth (Caluwé et al., 2016). Previous studies indicate that prolonged photoperiods can cause photoinhibition, a negative feedback mechanism that limits photosynthesis and growth to avoid damage to the photosynthetic apparatus when the plant receives more light than it can use (Takahashi & Badger, M., 2011). On the other side, short and frequent photoperiods have been shown to optimize photosynthetic productivity in annual species and microalgae (Zhang et al., 2019). However, little is known about the possible impacts of accelerated circadian cycles on carbon metabolism and growth of perennial crops, such as grapevine. Addressing the impact of circadian rhythm on grapevine functioning is thus necessary to determine the most efficient light conditions under indoor growing systems.

Microvine (*Vitis vinifera*) is a natural mutant that allows short experiments in fully controlled environment in growth chambers due to its small size, fast juvenile cycle and continuous fruiting (Torregrosa et al., 2019). Moreover, microvine varieties resistant to mildews, recently released from our breeding programs, considerably lower the use of chemicals, which is a pre requisite when working under confined spaces. Lastly, microvine vegetative development and individual berry growth and metabolism were shown to be very similar to grapevine (Luchaire et al., 2017; Torregrosa et al., 2019). Altogether, these properties make the microvine a suitable model for determining how changes in the circadian rhythm could impact the efficiency of grapevine functioning and resource requirements.

RESEARCH OBJECTIVES

This study assessed the impacts of an accelerated circadian rhythm of photoperiod (3-hour light/3-hour dark cycles) compared to standard circadian rhythm (12-hour light/12-hour dark cycles) on development, growth, metabolism and water use in two microvine genotypes of *Vitis vinifera*. It was also aimed at determining whether accelerated circadian cycles can avoid photoinhibition and improve photosynthesis rate, carbon gain and biomass allocation to reproductive organs. Ultimately, this study provides new information to optimize production of perennial fleshy fruit crops and resource requirements, through the control of circadian rhythm under artificial growth systems (growth chambers, greenhouse) in urban area.

MATERIAL AND METHODS

Experimental Conditions

The study was conducted in growth chambers on two-year-old potted microvines (Chaib et al., 2010), genotypes V3xG5 No. 16 and No. 102 (Breil et al., in prep). Plants were subjected to two circadian rhythm treatments: 12-h light/dark control cycle (PHOT 12/12) and 3-h light/dark accelerated cycle (PHOT 3/3). Climatic conditions were set as follow: temperature of 28°C/15°C (day/night), vapor pressure deficit (VPD) of 1 kPa/0.5 kPa (day/night) and photosynthetically active radiation (PAR) of 500 µmol m^{-2} s^{-1}, corresponding to a cumulated PAR over 24h of approximately 22 µmol m^{-2} day^{-1} for both treatments.

Plant Material

Prior to the starting of the experiment (T0), plants were grown in greenhouse until they reached approximately 48 unfolded leaves. All plants were trained to maintain a single proleptic axis, removing axillary shoots as soon as they appeared. At T0, all leaves and inflorescences older than plastochron index (PI = phytomer position from the apex) number 30, which held an inflorescence at flowering stage (ClusterFlow-T0), were removed.

The study was divided into two periods (P1, P2), based on the development stage of 'ClusterFlow-T0'. P1 and P2 corresponded respectively to the periods from flowering to veraison and from veraison to maximum berry volume of 'ClusterFlow-T0'. This latter stage marked the end of the trial (Tfinal).

Development, Growth and Resource Use

Leaf emergence rate was determined from weekly observations (P1 & P2) to calculate the average Phyllochron (Phyll) and its rate of variation over time (Slope Phyll). The individual leaf area (LAi) at each node position was estimated from main vein length measurements at the end of P1, using an allometric relationship (Luchaire et al., 2017). Maximum leaf area (a90) was calculated from a fitting adjustment of LAi as a function of growing degree days (GDD), inferred from the spatial patterns along the axis at the end of P1 as reported by Luchaire et al. (2017). The total plant leaf area (LA) was also determined from the sum of LAi.

Leaf disc samples (30 mm^{-2} diameter) were taken on young fully expanded leaves (PI=10) two times during P1. The leaf discs were dried in an oven at 60°C for 24 hours and weighed to calculate the Specific Leaf Area (SLA). At the end of P2 (Tfinal), vegetative organs (Veg. Organs: leaves, petioles and internodes) were dried in an oven (60°C) and reproductive organs (Reprod. Organs: inflorescences, bunches) were dehydrated by freeze-drying. The plant dry biomass (DMtotal) was determined from the sum of vegetative and reproductive organs DM. Lastly, the daily transpiration was determined from pot weight variations over 24h during P1, and the water and radiation use efficiency (WRUE) was estimated from the total biomass produced divided by the water used and PAR accumulated during the complete growth cycle (P1+P2). Photosynthesis dynamics and efficiency

Net photosynthesis rate (An) and dark respiration (Rd) were assessed with a portable photosynthesis system LI-6800 (LI-COR Inc., Lincoln, NE, USA) over 24 h on leaves at PI=10 and PI=11, respectively. An and Rd were measured five times during the day and night for PHOT 12/12 and three times during the day and night for PHOT 3/3. Daily carbon gain (DCgain) was then calculated by integrating the areas under the temporal An and Rd curves. Chlorophyll fluorescence measurements were performed at the end of the day (ED) and night (EN) to assess photosynthetic efficiency parameters including the photosystem II efficiency (φPSII), the electron transport rate (ETR), and the photochemical (qP) and non-photochemical (qN) quenching as described in Villalobos-González et al. (2022).

Carbohydrate and Nitrogen Leaf contents

Eight discs per leaf (PI = 10) per plant were sampled at the same time as the An measurements, six for the carbohydrate content assays (soluble solids and starch) and two for the total nitrogen (N) and carbon (C) content assays. All samples were freeze-dried. Soluble carbohydrates were extracted with ethanol, starch was extracted using amyloglucosidase in buffer solutions, then analyzed using a CLARIOstar® Plus multimode plate reader (BMG LABTECH, Ortenberg, Germany). Leaf nitrogen was measured with a Vario Pyro Cube automatic analyzer (Elementar, Lyon, France) and a mass spectrometer. The carbon: nitrogen (C:N) ratio was then determined.

Statistical analysis

The experimental design was completely randomized and factorial, evaluating the factors of treatment (circadian rhythm) and genotype. Analysis of variance (ANOVA) and post hoc tests were performed using the statistical software Jamovi. In addition, F-test analysis was used to compare the regressions of the growth dynamics, and principal component analysis (PCA) was used to evaluate patterns of variability and relationships between all variables at the leaf and plant scale.

RESULTS

Leaf growth and C/N metabolism (P1 period)

The maximal individual leaf area (a90) inferred from spatial pattern along the main axis was 39% higher for GENOT 102 compared to GENOT 16, and it was 23% higher for GENOT 16 under PHOT 3/3 compared to PHOT 12/12. Photosynthesis (An) was rather stable throughout the light period under PHOT 3/3 for both genotypes (Fig.1). In contrast, for both genotypes, plants under PHOT 12/12 showed a decrease (– 62%) at the end of the day period (ED). At the end of the night period (EN), the dark respiration (Rd) was lower (-51%) for PHOT 12/12 compared to PHOT 3/3 regardless the genotype. Ultimately the daily carbon gain (DCgain) was 66% higher in PHOT 3/3 compared to PHOT

12/12, and 20% higher for GENOT 102 compared to GENOT 16. In spite of these C gain variations, the total

leaf C content (TC) was similar between the treatments and genotypes. However, leaf N content was higher under PHOT 3/3 for both genotypes (+ 17% on average for EN and ED) compared to PHOT 12/12, resulting in a lower C:N ratio in PHOT 3/3 (-17% on average for EN and ED). Lastly, the SLA was 13.43 % higher in GENOT 102 than in GENOT 16, without differences between treatments.

A PCA representing the variables at leaf level is shown in Fig.2A. On axis 1 (45.29%), a90, DCgain and SLA were negatively related to C:N ratio. Axis 2 (23.09%) was represented by TC. Treatment and genotype were mainly spread on axis 1, with PHOT 3/3 and GENOT 102 being located most to the left side of the axis (greater a90, DCgain, thinner leaves (higher SLA) and lower C:N ratio) compared to PHOT 12/12 and GENOT 16.

Plant development, growth and resource use (P1 & P2 periods)

During the P1, the phyllochron (Phyll 1) was minimum and stable, ranging approximately 23 °Cd phytomer^{-1} in all treatments and genotypes. However, from the beginning of ripening of ClusterFlow-T0 berries onwards (P2), the rate of phyllochron increase (Phyll Slope 2) to 1 °Cd phytomer^{-1} per day. The total growth cycle in PHOT 3/3 was 7 days longer than in PHOT 12/12, mainly due to the extension of P1, while the duration of P2 (ripening phase) was similar in all treatments and genotypes. The total dry mass (DMtotal) at Tfinal reached 75 g for the two treatments. However, GENOT 102 showed a higher DMtotal (+38%) than GENOT 16. In addition, partition of DM to reproductive organs (% Repro. Organs) was higher (+15%) for in vegetative organs at the expense of partition of DM to vegetative organs (% Veg. Organs -26%) for GENOT 102 compared to GENOT 16. Lastly, no differences in water and radiation use efficiency (WRUE) were observed between treatments or genotypes.

A PCA including the variables at the plant level is shown in Fig.2B. On axis 1 (52.08% variability), DMtotal, % Repro. Organs and WRUE were opposite to % Veg. Organs. On axis 2 (17.88% variability), cycle length, Phyll Slope 2 and total leaf area (LA) were opposite to Phyll 1. Both genotypes (16 and 102) under PHOT 12/12 were grouped in the central part of the PCA, indicating an intermediate response in the evaluated variables. However, the PHOT 3/3 treatment for GENOT 102 was located towards the left side axis 1 related to higher DMtotal, % Repro. Organs and WRUE and GENOT 16 under PHOT 3/3 was positioned at the top of axis 2, standing out for longer cycle duration, higher Phyll Slope 2 and LA.

CONCLUSION

Accelerating the circadian cycle in microvines favored growth and daily carbon gain, due to the maintenance of An rates and lower Rd. In addition, GENOT 102 proved to be more efficient than GENOT 16 in terms of daily carbon gain, total DM produced and higher allocation of DM towards reproductive organs in the same 95-day period, a tendency that was accentuated under PHOT 3/3. This indicates that accelerated circadian photoperiod cycles and genotype selection can help optimize perennial crop production without affecting metabolic processes during maturation. These techniques offer an alternative for urban agriculture and crop management in confined environments.

ACKNOWLEDGEMENTS

The authors thank Myriam Dauzat and Stephane Berthezene of the Montpellier Plant Phenotyping Platform (M3P) PhenoPsis for helping with growth chamber monitoring and Gaelle Rolland for accompanying biochemical assays.

REFERENCES

Caluwé, J., Xiao, Q., Hermans, C., Verbruggen, N., Leloup, J., & Gonze, D. (2016). A compact model for the complex plant circadian clock. Frontiers in Plant Science, 7. https://doi.org/10.3389/fpls.2016.00074.

Chaib, J., Torregrosa, L., Mackenzie, D., Corena, P., Bouquet, A., & Thomas, M. R. (2010). The grape microvine – a model system for rapid forward and reverse genetics of grapevines. Plant Journal, 61, 1083–1092. https://doi.org/10.1111/j.1365-313X.2010.04219.

Luchaire, N., Rienth, M., Romieu, C., Nehe, A., Chatbanyong, R., Houel, C., Ageorges, A., Gibon, Y., Turc, O., Muller, B., Torregrosa, L., & Pellegrino, A. (2017). Microvine: A new model to study grapevine growth and developmental patterns and their responses to elevated temperature. American Journal of Enology and Viticulture, 68(3), 283–292. https://doi.org/10.5344/ajev.2017.16066.

Muluneh, M. (2021). Impact of climate change on biodiversity and food security: A global perspective - A review article. Agriculture & Food Security, 10, 1–25. https://doi.org/10.1186/s40066-021-00318-5.

Paradiso, R., & Proietti, S. (2021). Light-quality manipulation to control plant growth and photomorphogenesis in greenhouse horticulture: The state of the art and the opportunities of modern LED systems. Journal of Plant Growth Regulation, 41, 742–780. https://doi.org/10.1007/S00344-021-10337-Y.

Takahashi, S., & Badger, M. (2011). Photoprotection in plants: A new light on photosystem II damage. Trends in Plant Science, 16(1), 53–60. https://doi.org/10.1016/j.tplants.2010.10.001.

Torregrosa, L., Rienth, M., Romieu, C., & Pellegrino, A. (2019). The microvine, a model for studies in grapevine physiology and genetics. OENO One, 53(3), 373–391. https://doi.org/10.20870/oeno-one.2019.53.3.2409.

Villalobos-González, L., Alarcón, N., Bastías, R., Pérez, C., Sanz, R., Peña-Neira, Á., & Pastenes, C. (2022). Photoprotection Is Achieved by Photorespiration and Modification of the Leaf Incident Light, and Their Extent Is Modulated by the Stomatal Sensitivity to Water Deficit in Grapevines. Plants, 11. https://doi.org/10.3390/plants11081050.

Zhang, X., Yuan, H., Guan, L., Wang, X., Wang, Y., Jiang, Z., Cao, L., & Zhang, X. (2019). Influence of photoperiods on microalgae biofilm: Photosynthetic performance, biomass yield, and cellular composition. Energies. https://doi.org/10.3390/en12193724.

FIGURES

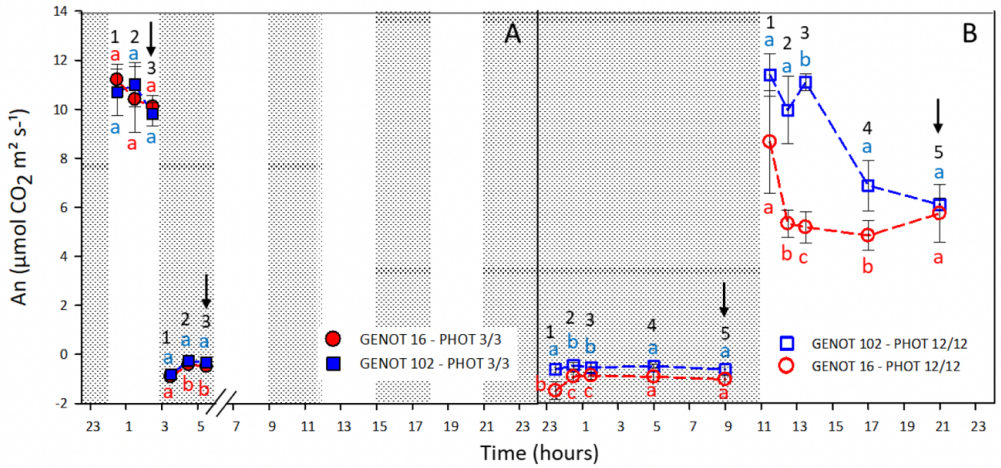

Figure 1. Dynamics of An and Rd of both genotypes under PHOT 3/3 treatment (A) and under PHOT 12/12 treatment (B) measured during P1. The circles numbered from 1 to 5 represent the dynamic measurement points over time. The letters indicate significant differences between treatments and genotypes at each measurement point (comparisons within the same measurement point). The arrows indicate the measurement points at the end of the day and the end of the night.

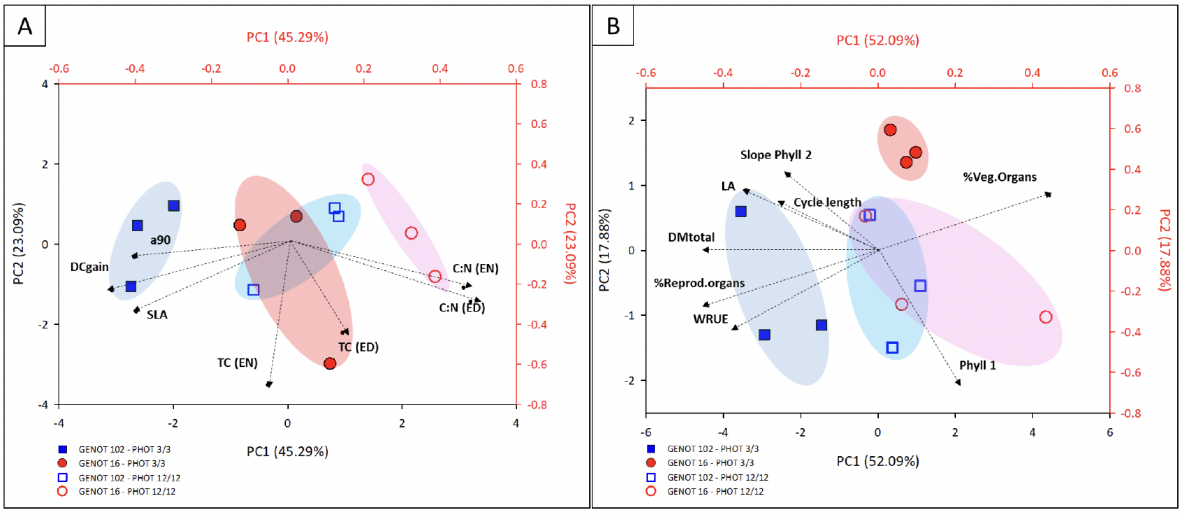

Figure 2. PCA analysis of variables at leaf level (A) and plant level (B) for each genotype-treatment combination. The graph shows the distribution of the different genotype-treatment combinations (GENOT 16-PHOT 3/3, GENOT 16-PHOT 12/12, GENOT 102-PHOT 3/3 and GENOT 102-PHOT 12/12) in the space of the first two principal components (PC1 and PC2). The loading scale is displayed in red and the scores scale in black. Variables at leaf level were measured during P1 and include DC gain (mol CO2 m^{-2} Day^{-1}), net daily carbon gain; a90 (cm^2): 90% of the maximum leaf size; SLA (mm^2 mg^{-1}), specific leaf area; TC (EN) and TC (ED), total carbohydrate content in leaves (mg carbohydrates. g DM^{-1}) at the end of the day (ED) and beginning of the day (BD) respectively; C:N (EN) and C:N (ED), C:N ratio at the leaf level ED and BD respectively. The plant-level variables were obtained at the end of P2 (Tfinal), except for LA and Phyll 1, which were obtained at the end of P1. Variables at the plant level are WRUE (mg DM/L/mol.m^{-2}), water and radiation use efficiency; Cycle length (Days), cycle length from T0 to Tfinal; %Veg.Organs, percentage of dry mass destined for the production of vegetative organs (leaves, stem and petioles); %Clusters, percentage of dry mass destined for the production of clusters of the total dry mass produced from T0 to Tfinal; DM total (g $plant^{-1}$), total DM produced per plant during P1 and P2 ; LA (cm^2 $plant^{-1}$), leaf area per plant of Leaves that grown in AB period, Phyll 1 (°C.d .$phytomer^{-1}$), mean phyllochron in P1; Slope Phyll 2 (Phyll day^{-1}), slope of the variation of the phyllochron as a function of time during P2.